Pergamon

Int. J. Heat Mass Transfer. Vol. 38, No. 10, pp. 1831–1840, 1995

0017–9310/95 $9.50+0.00

0017–9310(94)00304–1

A heat balance integral model of the thermistor

A. S. WOOD and S. KUTLUAY
University of Bradford, Department of Mathematics, Bradford, West Yorkshire BD7 1DP, U.K.

(*Received* 14 *April* 1993 *and in final form* 6 *September* 1994)

Abstract—A simplified model of one particular thermistor is presented and an approximate functional solution for the evolving coupled thermo-electric problem is obtained by an application of the heat balance integral method. The solution is shown to exhibit all the correct physical characteristics and this simple model extracts a mechanism by which the observed cracking of these devices might be initiated.

1. INTRODUCTION

The thermistor is a ceramic thermo-electric device which may form one element of an electric circuit. The basis for its operation is an electrical conductivity G that is a highly non-linear function of the temperature T, typically decreasing by five orders of magnitude as the temperature rises over a relatively small critical range, say 100–200°C. This is a positive temperature coefficient device (PTC). The behaviour of G makes the thermistor useful in many areas some of which are thermometry, the measurement of microwave-frequency power, thermal relays and control devices activated by changes in temperature such as a current-surge protector [1]. Comprehensive details of the properties, operation and applications of the PTC thermistor are available in the literature [1, sections 9–12] and here we limit ourselves to a schematic description of its behaviour.

The current flowing through the device drives internal Joule heating. From Ohm's law, a larger current produces greater heating and so an enhanced temperature increase in certain regions of the device. In this way, more of the ceramic material rises above the critical temperature range (the hot region) and the bulk electrical conductivity falls. There is a subsequent decrease in the current flowing through the device which in turn reduces the Joule heating. At some point a thermal equilibrium is attained in which the heating is balanced by the loss of heat at the surface of the device. Gelder and Guy [2] discuss the opposite case of low resistivity at higher temperatures and investigate the use of certain glass products in thermal switching devices.

During the last five years or so considerable interest has been shown in the thermistor, much of which has been motivated by the fact that, during their operation, these devices have been observed to develop cracks. This is likely to affect their operational behaviour and one obvious hypothesis is that large heat fluxes occur during the working life of the device. There is conflicting evidence of this. Veen's [3] numerical experiments displayed no such high fluxes. However, under certain conditions, the resistivity of the device can combine with the resistance of the external circuit to produce temperature surges within the device [4, 5]. The resulting thermal stresses may induce cracking.

Of practical interest is a knowledge of the evolution of the moving boundary separating the hot region from the cold region (below the critical temperature). It is the purpose of this paper to construct and assess a simple functional approximation for tracking the moving boundary and the associated thermo-electric distributions. For the thermal problem there is a fairly small but detailed reference list. Diesselhorst [6] gave proofs for the existence and uniqueness of solutions for the problem consisting of isothermal/isopotential conditions on the upper and lower faces with thermo-electric insulation at the sides of the device. Howison [7] constructed some order results for the size of the hot region and showed [8] that the results were essentially independent of the geometry of the device. Cimatti [9] completed the uniqueness proof, giving a classical solution, and in an earlier paper [10] obtained an upper bound for the temperature in the case of uniform Dirichlet boundary conditions on the entire surface of the device.

More realistically the surface of the device admits Robin's thermal boundary conditions and Westbrook [11] used an iterative method based on finite elements to obtain numerical results for the isotherm locations and field lines in the steady-state situation. The thin hot strip lying in a radial direction at the centre of the device, produced by his scheme, agreed with the previous order analysis [7]. A numerical process to follow the evolving thermal profile in a one-dimensional analogue has been summarised [12] as has interaction with an external circuit [3].

The heat balance integral solution presented in this paper not only exhibits all the correct physical characteristics of the problem but, in addition, correctly predicts the physical *a priori* conditions defining the steady-state configurations [11]. Although the problem of crack propagation is not addressed, we do show

NOMENCLATURE

Bi	Biot number
E	Young's modulus [N m^{-2}]
G	electrical conductivity [S]
g	dimensionless electrical conductivity
l	thermistor half length [m]
S	hot–cold interface location [m]
s	dimensionless hot–cold interface location
T	temperature [°C]
t	dimensionless time
U	dimensionless temperature
V	applied potential difference [V]
Y	axial distance [m]
y	dimensionless axial distance.

Greek symbols

α	surface heat transfer coefficient [W m^{-2} K^{-1}]
γ	coefficient of thermal expansion [K^{-1}]
δ	scale factor for electrical conductivity
ΔT	temperature difference $T_c - T_a$ [K]
ε	scale factor for electrical conductivity
κ	thermal diffusivity [m^2 s^{-1}]
λ	thermal conductivity [W m^{-1} K^{-1}]
ν	Poisson's ratio
σ	tensile strength [N m^{-2}]
τ	time [s]
Φ	electric potential [V]
ϕ	dimensionless electric potential
ω	ratio of heating terms.

Subscripts

0	end of cold phase
1	end of warm phase
a	ambient (air) value
c	critical (switching) value.

Superscript

*	steady-state value.

that rates of temperature change commensurate with crack-inducing thermal stresses can take place at intervals during the process evolution.

2. STATEMENT OF THE PROBLEM

We assume a right-circular cylindrical form for the device. Current flow is driven by applying a potential $\Phi = \pm V$ at the upper and lower (plane) faces. If the curved sides are electrically insulated then current flows in the axial direction only. The internal Joule heating causes heat to flow towards the edges where it is liberated to the surrounding medium (air). If the curved sides of the device are also perfectly insulated with respect to heat flow then the entire thermo-electric problem is one-dimensional in the axial direction. Heat loss at the upper and lower faces is identical and so, about the centre point, there is symmetry in T and skew-symmetry in Φ. Introducing the dimensionless variables

$$U = \frac{T - T_a}{\Delta T}, \quad y = \frac{Y}{l}, \quad s = \frac{S}{l},$$

$$t = \frac{\kappa\tau}{l^2}, \quad \phi = \frac{\Phi}{V} \quad \text{and} \quad g = \frac{G}{G_a}$$

then we need only consider the dimensionless region $0 \leqslant y \leqslant 1$.

2.1. *Heat flow*

The temperature U is governed by the diffusion equation

$$\frac{\partial U}{\partial t} = \frac{\partial^2 U}{\partial y^2} + \omega g\left(\frac{\partial \phi}{\partial y}\right)^2, \quad 0 \leqslant y \leqslant 1, \quad t > 0. \quad (1)$$

The second term on the right-hand side of (1) represents the effect of Joule heating in which $\omega = G_a V^2/\lambda\Delta T$ is a dimensionless quantity expressing the ratio of electric heating to heat conduction and g is temperature dependent and initially ($t = 0$) equals 1. To model its non-linear behaviour we assume that above some unique critical temperature, $U_c = 1$, its value drops to δ where, typically, $\delta = 10^{-5}$. Thus,

$$g(U) = \begin{cases} 1, & 0 \leqslant U \leqslant 1, \\ \delta, & U > 1. \end{cases} \quad (2a)$$

In a postscript, Howison [7] notes that the step function is not the most realistic model for g and that an exponential rule, of the form

$$g(U) = \exp\left(\frac{-f(U)}{\varepsilon}\right)$$

$$f(U) = \begin{cases} 1, & 0 \leqslant U \leqslant 1 \\ U-1, & 1 < U < 1+\Delta U \\ 1, & U \geqslant 1+\Delta U \end{cases} \quad (2b)$$

is more appropriate where, typically, $\varepsilon \sim 10^{-1}$ and $\Delta U = 1$. This point is also asserted in [1, pp. 178–182]. However, for the step function, we can generate a functional solution to the thermistor problem relatively easily, which we shall compare with a numerical solution of the full problem using the definitions in (2b).

The initial temperature of the device equals the ambient (air) temperature,

$$U(y, 0) = 0, \quad 0 \leqslant y \leqslant 1 \quad (3)$$

by symmetry the plane $y = 0$ has no heat flow across it,

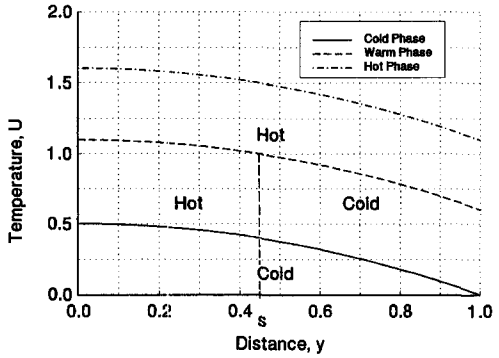

Fig. 1. Steady-state configurations.

$$\frac{\partial U}{\partial y} = 0, \quad y = 0, \quad t > 0 \tag{4}$$

and at $y = 1$ heat is lost to the surroundings,

$$\frac{\partial U}{\partial y} + Bi\, U = 0, \quad t > 0 \tag{5}$$

in which $Bi = \alpha l/\lambda$ is a Biot number. For the given initial conditions in equation (3) and with $Bi > 0$, we assume monotonicity of the temperature profile such that the point $y = 0$ will always be the hottest and will be the first point to reach the temperature U_c. Ultimately the rate of heat loss at $y = 1$ will equal the rate of internal heat generation and equilibrium will be attained which may be any one of the three scenarios shown in Fig. 1.

During the warm phase there are two distinct regions, i.e. a hot region $0 \leqslant y \leqslant s^*$ (at a temperature above U_c) of low electrical conductivity separated by a free boundary s^* from a cold region (at a temperature below U_c) of high electrical conductivity. The evolving problem defined by equations (1)–(5), using the step condition (2a), will move sequentially through the cold, warm and hot phases (if at all). Three distinct phases are observable, each having a slightly different model.

2.2. *Current flow*

Coupled with the evolving temperature is an implicitly time dependent potential ϕ, initially assumed to have the profile $\phi(y,0) = y$ and subsequently governed by

$$\frac{\partial}{\partial y}\left(g\frac{\partial \phi}{\partial y}\right) = 0, \quad 0 < y < 1, \quad t > 0 \tag{6}$$

$$\phi(0,t) = 0, \quad t > 0 \tag{7}$$

$$\phi(1,t) = 1, \quad t > 0. \tag{8}$$

3. AVAILABLE SOLUTIONS

Equations (6)–(8) can be solved exactly for the three phases and the ultimate problem is to track the evolving temperature profiles.

3.1. *Cold phase*: $0 \leqslant t \leqslant t_0$

The entire region is at a temperature no greater than U_c and so $g = 1$. Hence $\phi(y,t) = y$, $0 \leqslant y \leqslant 1$, $\partial\phi/\partial y = 1$ and equation (1) becomes

$$\frac{\partial U}{\partial t} = \frac{\partial^2 U}{\partial y^2} + \omega, \quad 0 < y < 1 \tag{9}$$

supplemented by the conditions (3)–(5). Equation (9) has the exact solution

$$U(y,t) = \omega\left(\tfrac{1}{2} + \frac{1}{Bi} - \frac{y^2}{2}\right) - 2\omega\, Bi \sum_{n=1}^{\infty} \frac{\cos(\mu_n y)}{\mu_n^2[\mu_n^2 + (Bi)^2 + Bi]\cos\mu_n} e^{-\mu_n^2 t}, \quad 0 \leqslant y \leqslant 1, \quad t \geqslant 0 \tag{10}$$

in which the μ_n are the positive roots of $\mu\tan\mu - Bi = 0$ [13]. Equation (10) may be used to assess the heat balance solution during the cold phase. At a time t_0, the value of $U(0,t)$ reaches U_c and the domain $0 \leqslant y \leqslant 1$ splits into two regions.

3.2. *Warm phase*: $t_0 < t \leqslant t_1$

There is now a hot region, $0 \leqslant y < s(t)$, at a temperature above U_c and a cold region, $s(t) \leqslant y \leqslant 1$, at a temperature no greater than U_c. The moving boundary $s(t)$ separates these two regions and equation (2a) defines the electrical conductivity within them.

3.2.1. *Hot region*: $0 \leqslant y \leqslant s(t)$. The solution to equation (6), subject to condition (7) and $\phi(s,t) = \bar{\phi}$, is

$$\phi(y,t) = \frac{\bar{\phi} y}{s}, \quad 0 \leqslant y \leqslant s(t) \tag{11}$$

where $\bar{\phi}$ is the value of the potential at $y = s(t)$. Further, $\partial\phi/\partial y = \bar{\phi}/s, g = \delta$ and equation (1) becomes

$$\frac{\partial U}{\partial t} = \frac{\partial^2 U}{\partial y^2} + \omega\delta\left(\frac{\bar{\phi}}{s}\right)^2, \quad 0 < y < s(t) \tag{12}$$

subject to

$$\frac{\partial U}{\partial y} = 0 \text{ at } y = 0 \quad \text{and} \quad U = 1 \text{ at } y = s(t). \tag{13}$$

The initial condition for equation (12) is obtained from the spatial distribution of U, arising from equation (10), at time t_0.

3.2.2. *Cold region*: $s(t) \leqslant y \leqslant 1$. The solution to equation (6), subject to $\phi(s,t) = \bar{\phi}$ and condition (8), is

$$\phi(y,t) = \frac{y(1-\bar{\phi}) + \bar{\phi} - s}{1-s}, \quad s(t) \leqslant y \leqslant 1. \tag{14}$$

Thus, $\partial\phi/\partial y = (1-\bar{\phi})/(1-s)$, $g = 1$ and equation (1) becomes

$$\frac{\partial U}{\partial t}=\frac{\partial^2 U}{\partial y^2}+\omega\left(\frac{1-\bar{\phi}}{1-s}\right)^2, \quad s(t)<y<1 \tag{15}$$

subject to

$$U=1 \text{ at } y=s(t) \quad \text{and} \quad \frac{\partial U}{\partial y}+Bi\,U=0 \quad \text{at} \quad y=1. \tag{16}$$

The initial condition for U again originates from equation (10).

3.2.3. *Potential* $\bar{\phi}$(t). The quantities $s(t)$ and $\bar{\phi}(t)$ are related. At $y=s(t)$ we assume continuity of potential gradient,

$$\delta\left.\frac{\partial \phi}{\partial y}\right|_{s^-}=\left.\frac{\partial \phi}{\partial y}\right|_{s^+}$$

and using the solutions (11) and (14) obtain

$$\bar{\phi}=\frac{s}{\delta+(1-\delta)s} \tag{17}$$

in which $s\in[0,1]\Rightarrow\bar{\phi}\in[0,1]$, $s(t_0)=0$ and $s(t_1)=1$. In equations (12) and (15),

$$\left(\frac{\bar{\phi}}{s}\right)=\frac{1}{\delta+(1-\delta)s} \quad \text{and} \quad \left(\frac{1-\bar{\phi}}{1-s}\right)=\frac{\delta}{\delta+(1-\delta)s}.$$

The denominator is positive for all $s\in[0,1]$ and so the heating terms are bounded.

3.3. *Hot phase*: t > t_1

Now $s(t)=1$ and all points $y\in[0,1]$ are above U_c. Also, $g=\delta$ and the solution to equations (6)–(8) is $\phi(y,t)=y$, $0\leqslant y\leqslant 1$. Thus, $\partial\phi/\partial y=1$ and equation (1) becomes

$$\frac{\partial U}{\partial t}=\frac{\partial^2 U}{\partial y^2}+\omega\delta, \quad 0<y<1 \tag{18}$$

subject to the boundary conditions (4) and (5). The initial condition is described, at $t=t_1$, by the spatial distribution of U at the end of the warm phase. In theory there exists a Fourier-type solution to this problem. However, in practice, the unknown form of the temperature profile at the end of the warm phase precludes an analytic determination of the Fourier coefficients.

3.4. *Interface* s(t)

We still have to track $s(t)$. With no latent heat of fusion, characteristic of phase-change problems, the usual Stefan condition is not available to drive the interface. We have what is known as an implicit free-boundary problem [14]. For the present problem, the condition

$$U(s(t),t)=1, \quad t_0<t<t_1$$

can be used to determine an ordinary differential equation that governs the motion of $s(t)$ (Section 4).

3.5. *Steady-state solutions*

As indicated in Section 2.1, any one of the cold, warm or hot phases may contain the steady-state situation. The particular configuration is governed by the acceptable values of s (or $\bar{\phi}$), which are in turn determined by the relative values of ω, Bi and δ. In this case the dimensionless model described so far degenerates to the one-dimensional problem presented in [11] (with ω and Bi replaced by the symbols α and β_1, respectively). If $\omega\leqslant 2Bi/(2+Bi)$ we obtain the cold solution ($s^*=0$)

$$U^*(y)=\frac{\omega}{2}\left(1+\frac{2}{Bi}-y^2\right), \quad \phi^*(y)=y, \quad 0\leqslant y\leqslant 1. \tag{19}$$

Clearly, if $\omega\geqslant 2$ a hot region must appear no matter how large the cooling coefficient Bi. If $\omega\delta>Bi$ we obtain the hot solution ($s^*=1$)

$$U^*(y)=\frac{\omega\delta}{2}\left(1+\frac{2}{Bi}-y^2\right), \quad \phi^*(y)=y, \quad 0\leqslant y\leqslant 1. \tag{20}$$

If $\omega(2+Bi)>2Bi\geqslant 2\omega\delta$ we obtain the warm solution

$$U^*(y)=1+\frac{\omega\delta}{2}(\bar{\phi}^{*2}-\phi^{*2})$$

$$\phi^*(y)=\frac{\bar{\phi}^* y}{s^*}, \quad 0\leqslant y\leqslant s^* \tag{21}$$

and

$$U^*(y)=1+\frac{\omega}{2}(\bar{\phi}^{*2}-\phi^{*2})$$

$$\phi^*(y)=\frac{(1-\bar{\phi}^*)y+\bar{\phi}^*-s^*}{1-s^*}, \quad s^*\leqslant y\leqslant 1 \tag{22}$$

in which $s^*\in(0,1]$ and $\bar{\phi}^*\in(0,1]$ are the steady-state values of $s(t)$ and $\bar{\phi}(t)$. Continuity of the potential gradient at s^* yields the relation

$$s^*=\frac{\bar{\phi}^*\delta}{1-(1-\delta)\bar{\phi}^*} \tag{23}$$

which necessarily implies continuity of the temperature gradient at $y=s^*$. Condition (5) yields the quadratic equation

$$(\bar{\phi}^*)^2+\frac{2}{Bi}(1-\delta)\bar{\phi}^*+\frac{2}{\omega}-1-\frac{2}{Bi}=0$$

from which $\bar{\phi}^*$, and hence s^* [equation (23)], can be evaluated in the case of a warm steady-state.

4. A HEAT BALANCE INTEGRAL SOLUTION

The heat balance integral (HBI) method [15] aims to construct a solution that satisfies the governing differential equations in an 'average' sense over the entire solution domain. The approach has been used to obtain small-time solutions for multi-dimensional

Stefan problems [16, 17]. Higher precision may be obtained by using sub-division of the solution domain [18].

The HBI solutions are constructed by assuming a quadratic form for the temperature profile that satisfies both boundary conditions and an integral form of the governing conduction equation. An appropriate quadratic satisfying conditions (4) and (5) is

$$U(y,t) = a\left(y^2 - 1 - \frac{2}{Bi}\right) \tag{24}$$

in which a is a function of time (to be determined).

4.1. *Cold phase*: $0 \leqslant t \leqslant t_0$

Integrating equation (9) over $0 \leqslant y \leqslant 1$ we obtain the heat balance integral

$$\int_0^1 \frac{\partial U}{\partial t}\,dy = \left[\frac{\partial U}{\partial y}\right]_0^1 + \omega$$

and, utilizing equation (24), can generate a first-order ordinary differential equation (ODE) for a,

$$-\frac{2(Bi+3)}{3Bi}\frac{da}{dt} - 2a = \omega \tag{25}$$

subject to $a(0) = 0$ [equation (3)]. Equation (25) can be solved exactly to give

$$U(y,t) = \frac{\omega}{2}\left(\exp\left[-\frac{3Bi\,t}{Bi+3}\right] - 1\right) \times \left(y^2 - 1 - \frac{2}{Bi}\right), \quad 0 \leqslant y \leqslant 1. \tag{26}$$

The boundary temperatures

$$U(0,t) = \frac{\omega(Bi+2)}{2Bi}\left(1 - \exp\left[-\frac{3Bi\,t}{Bi+3}\right]\right)$$

and $$U(1,t) = \frac{2}{Bi+2}U(0,t)$$

satisfy the physical requirement that $U(0,t) > U(1,t)$. Further

$$\lim_{t\to\infty} U(0,t) = \frac{\omega(Bi+2)}{2Bi}.$$

An all cold steady-state solution exists only if this expression is bounded by U_c, i.e. if $\omega \leqslant 2Bi/(Bi+2)$. This is precisely the condition given in ref. [11] and (26) then takes the form of the exact steady-state solution (19).

If $\omega > 2Bi/(Bi+2)$ then $U(0,t)$ will reach $U_c = 1$ in a time

$$t_0 = -\left(\frac{Bi+3}{3Bi}\right)\ln\left(1 - \frac{2Bi}{\omega(Bi+2)}\right)$$

with an associated temperature distribution

$$U(y,t_0) = 1 - \frac{Bi\,y^2}{Bi+2}, \quad 0 \leqslant y \leqslant 1, \quad U(1,t_0) = \frac{2}{Bi+2}.$$

4.2. *Warm phase*: $t_0 < t \leqslant t_1$

Using the heat equations (12) and (15) and integrating over $0 \leqslant y \leqslant 1$ we obtain

$$\int_0^1 \frac{\partial U}{\partial t}\,dy = \left[\frac{\partial U}{\partial y}\right]_0^1 + \frac{\int_0^s \omega\delta\,dy + \int_s^1 \omega\delta^2\,dy}{(\delta + (1-\delta)s)^2}.$$

Substitution of the profile equation (24) gives the ODE

$$-\frac{2(Bi+3)}{3Bi}\frac{da}{dt} - 2a = \frac{\omega\delta}{\delta + (1-\delta)s}. \tag{27}$$

The time dependence of s renders impossible the determination of a particular solution for this equation and so we use a numerical procedure (Section 5). The boundary condition $U(s(t),t) = 1$ implies

$$a = \frac{1}{s^2 - 1 - \frac{2}{Bi}} \tag{28}$$

and, with the change of variable $z = s^2$, equation (27) is transformed into an equation for the moving boundary

$$\frac{dz}{dt} = p(z) \quad z(t_0) = 0 \tag{29}$$

in which

$$p(z) = \frac{3Bi}{2(Bi+3)}\left(z - 1 - \frac{2}{Bi}\right) \times \left[2 + \frac{\omega\delta}{\delta + (1-\delta)\sqrt{z}}\left(z - 1 - \frac{2}{Bi}\right)\right].$$

At any time, $s = \sqrt{z}$, $\dot{s} = \dot{z}/2s$, $\dot{} \equiv d/dt$ and a is given by (28). Thus, a complete description of the thermal behaviour is available until either (i) a steady-state situation is reached in which $\lim_{t\to\infty} s \in (0,1)$ or (ii) s becomes equal to 1 and the problem enters a hot phase. A steady-state will occur if $\dot{s}$, and hence $\dot{z}$, equals zero. From equation (29) we obtain

$$s^* = \left(\frac{1-\delta}{\omega\delta}\right)\left[-1 \pm \left\{1 - \frac{\omega\delta^2}{(1-\delta)^2} \times \left(2 - \frac{\omega(Bi+2)}{Bi}\right)\right\}^{1/2}\right].$$

Clearly $s^* > 0$, since $\omega > 2Bi/(Bi+2)$, and $1-\delta > 0$ so we take the positive root. The inequality $s^* \leqslant 1$ leads to the necessary condition $\omega\delta \leqslant Bi$ and so the conditions for a warm steady-state configuration agree with [11].

If $\omega\delta > Bi$, $s(t)$ becomes equal to 1 at a time t_1 [obtained numerically from equation (29)] and the entire region becomes hot in the steady-state limit. We have $a(t_1) = -Bi/2$ from which $U(0,t_1) = 1 + Bi/2$, $\dot{U}(1,t_1) = 1$ and

$$U(y,t_1) = -\frac{Bi}{2}\left(y^2 - 1 - \frac{2}{Bi}\right), \quad 0 \leqslant y \leqslant 1. \quad (30)$$

4.3. *Hot phase*: $t > t_1$

Integrating equation (18) over $0 \leqslant y \leqslant 1$ and using the profile equation (24), the HBI method gives a similar ODE to that of the cold phase [equation (25)] with ω replaced by $\omega\delta$:

$$-\frac{2(Bi+3)}{3Bi}\frac{da}{dt} - 2a = \omega\delta.$$

The general solution is

$$U(y,t) = \left(k\exp\left[-\frac{3Bi\,t}{Bi+3}\right] - \frac{\omega\delta}{2}\right) \times \left(y^2 - 1 - \frac{2}{Bi}\right), \quad 0 \leqslant y \leqslant 1. \quad (31)$$

At $t = t_1$ the warm and hot solutions, equations (30) and (31), must be continuous, from which the constant k can be found giving

$$U(y,t) = \frac{1}{2}\left((\omega\delta - Bi)\exp\left[-\frac{3Bi(t-t_1)}{Bi+3}\right] - \omega\delta\right) \times \left(y^2 - 1 - \frac{2}{Bi}\right), \quad 0 \leqslant y \leqslant 1.$$

The boundary temperatures are

$$U(0,t) = \left(\frac{Bi+2}{2Bi}\right)\left(\omega\delta - (\omega\delta - Bi) \times \exp\left[-\frac{3Bi(t-t_1)}{Bi+3}\right]\right), \quad U(1,t) = \frac{2}{Bi+2}U(0,t)$$

and the hot steady-state form is identical to the exact profile equation (20).

5. NUMERICAL EXPERIMENTS AND DISCUSSION

It is a simple matter to choose values of ω, Bi and δ and to evaluate the temperature profiles of Section 4. We shall use a value of $\delta = 10^{-5}$ in the numerical simulations of this section. The only complications that may arise will be in solving equation (29) numerically (if a warm phase exists).

We shall compare the HBI solution to the problem tackled by Fowler *et al.* [5] which uses equation (2b) to define the electrical conductivity. In order that $g(U) = \delta$ for $U > 1 + \Delta U$, to be consistent with the step function (2a), we use the value

$$\varepsilon = \frac{0.2}{\ln 10} (\simeq 0.087).$$

In ref. [5] the value $\Delta U = 1$ is used. To summarise their one-dimensional model, integrating equation (6) with respect to y gives

$$\frac{\partial\phi}{\partial y} = \frac{c(t)}{g}. \quad (32)$$

A further integration produces

$$\phi(y,t) = \int_0^y \frac{c}{g}\,dy = c(t)\int_0^y \exp\left(\frac{f(U)}{\varepsilon}\right)dy$$

and since $\phi(1,t) = 1$, for all $t > 0$, then

$$c(t) = \left[\int_0^1 \exp\left(\frac{f(U)}{\varepsilon}\right)dy\right]^{-1}.$$

Using equation (32), the governing heat flow equation (1), becomes

$$\frac{\partial U}{\partial t} = \frac{\partial^2 U}{\partial y^2} + \omega c^2 \exp\left(\frac{f(U)}{\varepsilon}\right), \quad 0 < y < 1, \quad t > 0. \quad (33)$$

It is a simple matter to construct an explicit numerical solution scheme based on finite differences, namely

$$u_i^{m+1} = u_i^m + \Delta t\,\dot{u}_i^m,$$

$$\dot{u}_i^m = \frac{u_{i+1}^m - 2u_i^m + u_{i-1}^m}{(\Delta y)^2} + \omega c^2 \exp\left(\frac{f(u_i^m)}{\varepsilon}\right).$$

The interval $0 \leqslant y \leqslant 1$ is divided into n equal cells of size $\Delta y = 1/n$, Δt is a time step and $u_i^m \simeq U(y_i, t_m)$. The value of Δt is determined by a heuristic stability argument based on ensuring positive values of $\partial U/\partial t$. The value of ΔU is critical, and this aspect will be explored later in this section.

5.1. *HBI solution: cold steady-state*

For a cold steady-state solution the values $\omega = 0.1$, $Bi = 0.2$ suffice. Figure 2(a) shows the evolving temperature profile on $0 \leqslant y \leqslant 1$ and Fig. 2(b) shows the behaviour of the boundary temperatures.

These figures are typical of a problem evolving to a cold steady state. Different values of ω and Bi, still satisfying the inequality $\omega < 2Bi/(2+Bi)$, simply serve to alter the time taken to attain a practical steady state. Clearly there is no evidence of either high flux values or rapid rates of change of temperature that may initiate cracking. Indeed, $\max |\dot{U}(y,t)| = |\dot{U}(0,0)| = 3$, under cold steady-state conditions. This agrees with Veen's conclusions [3].

5.2. *HBI solution: warm steady-state*

The values $\omega = 0.5$ and $Bi = 0.2$ will give a warm steady-state. Figure 3(a) shows a similar evolving temperature profile to the cold problem with no evidence of high fluxes. Figures 3(b) and (c) show the evolving behaviour of the boundary temperatures, and clearly there are no particularly rapid changes in temperature. Once in the warm phase the solution reaches its steady-state extremely quickly, in a time $t = 2 \times 10^{-9}$, as compared to the duration of the cold phase, $t_0 = 2.4$. This reflects the behaviour of the interface $s(t)$ (and potential $\bar{\phi}$) shown in Fig. 3(d).

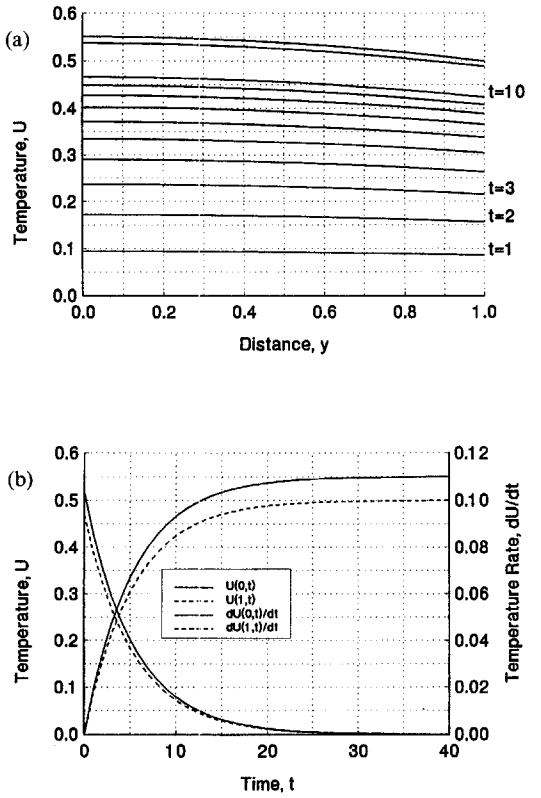

Fig. 2. (a) Temperature profile evolving to a cold steady-state and (b) evolving boundary temperatures.

The differential equation (29) was solved using Euler's method. The very fast initial speed $\dot{s}$ does not cause problems and the boundary $s(t)$ rapidly and smoothly reaches its steady-state value.

5.3. *HBI solution*: *hot steady-state*

The values $\omega = 100\,000$ and $Bi = 0.2$ give a hot steady-state. The temperature profiles shown in Fig. 4(a) again display small fluxes. However, the temperature changes during the cold phase, shown in Fig. 4(b), are extremely high. The gradients of the two lines are $\dot{U}(0,t) \simeq 1.03 \times 10^5$ and $\dot{U}(1,t) \simeq 0.94 \times 10^5$. Essentially the thermistors' entire temperature profile is 'lifted' very rapidly, i.e. a *temperature surge*. Clearly, here is a mechanism for initiating cracks in the ceramic crystal structure.

This rate of change rapidly tails off during the short warm phase [Fig. 4(c)] and we observe the expected exponential approach to a steady-state in the hot phase [Fig. 4(d)].

The rapid temperature changes seen above will cause stress build up in the micro-structure of the thermistor. The ceramic material of the thermistor is quite brittle and tends to suffer micro-structural cracks which will concentrate the thermal stresses and perhaps lead to crack propagation. Stress analysis shows that if thermal expansion is prevented while heating a ceramic body from a temperature T_A to a

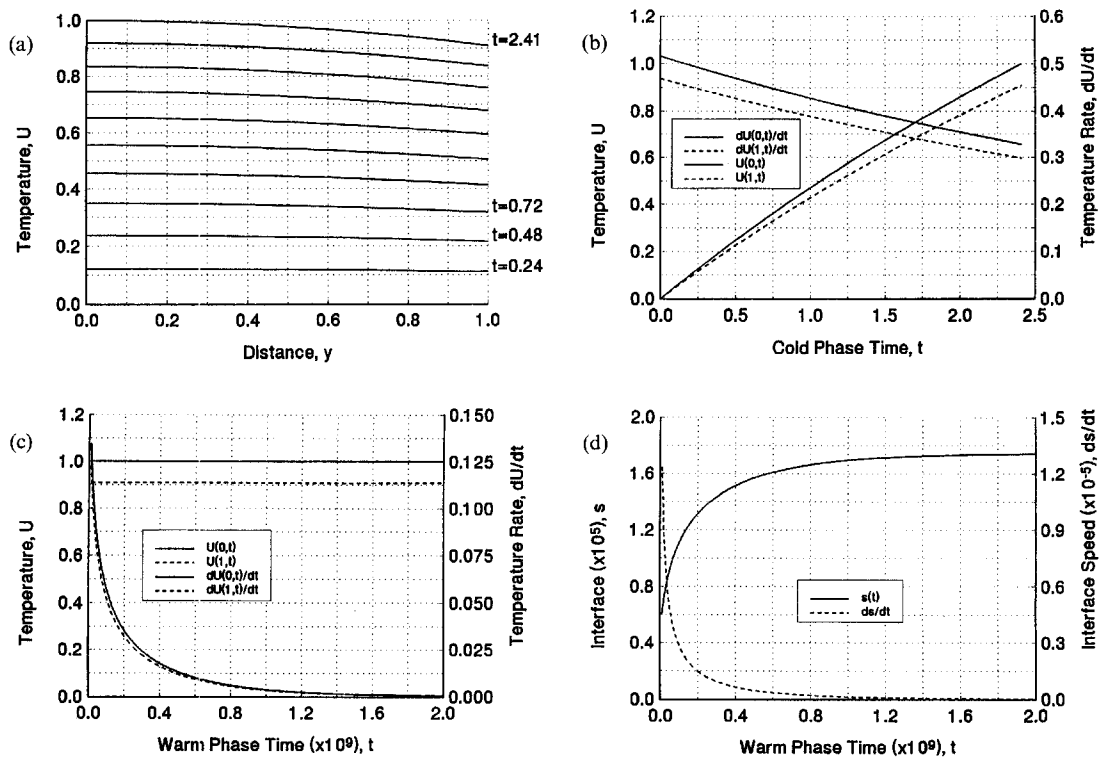

Fig. 3. (a) Temperature profile evolving to a warm steady-state, evolving boundary temperatures during (b) the cold phase, (c) the warm phase and (d) evolving interface location during the warm phase.

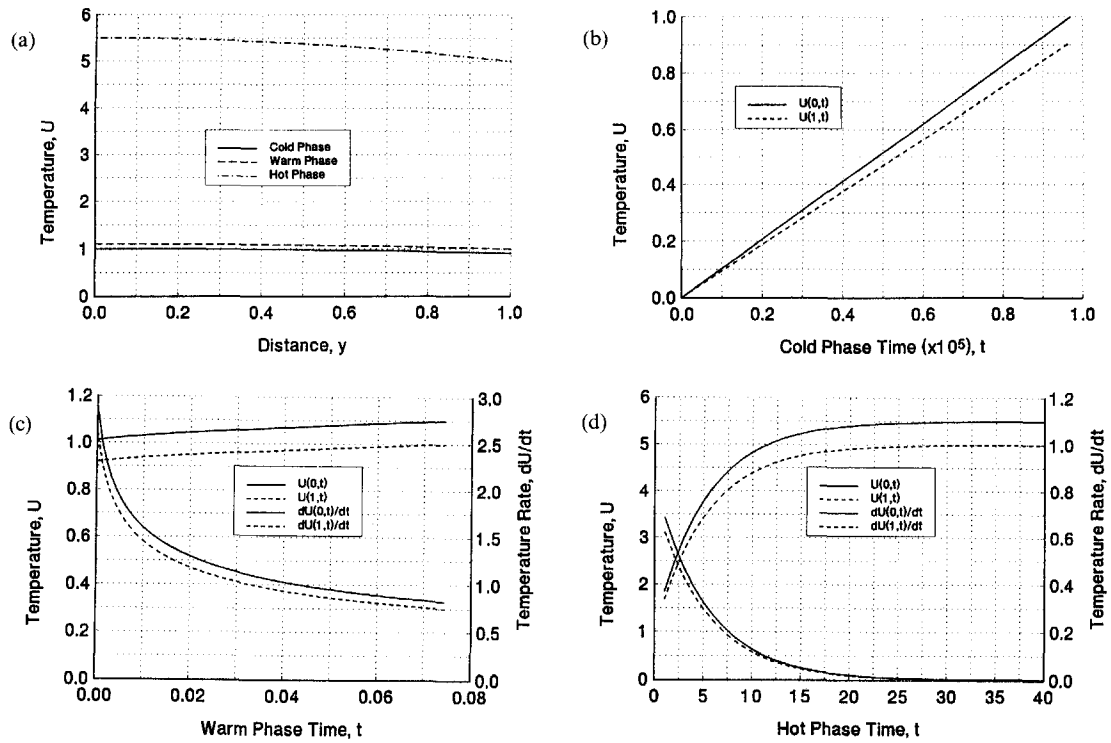

Fig. 4. (a) Temperature profile at end of cold, warm and hot phases, evolving to a hot steady-state, and evolving boundary temperatures during (b) cold phase, (c) warm phase and (d) hot phase.

temperature T_B then a compressive stress σ results given by [19]

$$\sigma = \frac{E_\gamma (T_B - T_A)}{1-\nu}.$$

If the fracture stress σ_f is known then the expression

$$\Delta T_f = \frac{\sigma_f (1-\nu)}{E_\gamma} \tag{34}$$

determines the largest rapid change in temperature that a material can withstand without suffering severe structural damage [19]. A typical PTC thermistor is made from barium titanate, $BaTiO_3$, which has the material properties $\sigma_f = 2.4\times10^7$ N m^{-2}, $\nu = 0.24$, $E = 2.4\times10^{10}$ N m^{-2}, $\gamma = 7\times10^{-6}$ K^{-1} and $\kappa = 1.6\times10^{-6}$ m^2 s^{-1}. Equation (34) gives a maximum temperature change of 108.6°C. For the above hot steady-state case, during the cold phase of duration $\Delta t = 9.7\times10^{-6}$, the temperature rises by $\Delta U = 1$. Using the change of variables of Section 2 and a typical thermistor half-length of $l = 4\times10^{-3}$ m, the cold phase lasts for

$$\Delta\tau = \frac{l^2 \Delta t}{\kappa} = 9.5\times10^{-5} \text{ s}.$$

If the ambient temperature is $T_a = 20$°C and the critical switching temperature is $T_c = 120$°C then the physical temperature increase is 100°C. Thus, thermal shock failure may occur, particularly if T_a is much less than 20°C.

5.4. *HBI step model vs Fowler's exponential model* [5]

In this section we make a brief comparison of the step and exponential models. The numerical scheme used $n = 10$ spatial cells of size $\Delta y = 1/10$. Appropriate results are presented in tabular form.

For the cold steady-state ($\omega = 0.1$, $Bi = 0.2$) there is little difference. This is not surprising since, for an all cold region $0 \leqslant y \leqslant 1$, $g(U) = 1$ for both models. We have already seen that the HBI solution approaches the analytic quadratic steady-state solution. The steady-state criterion requires both $|\dot{U}(y=0)| < \frac{1}{2}\times10^{-8}$ and $|\dot{U}(y=1)| < \frac{1}{2}\times10^{-8}$. Both numerical steady-state profiles agree with the exact formula (19) to seven decimal places. The only marked difference is the time to attain steady-state. For the HBI model, $t_\infty = 90$ and for the exponential model $t_\infty = 81$.

For a warm steady-state ($\omega = 0.5$, $Bi = 0.2$) both models provide very similar predictions for the time at which the cold phase ends (t_0(HBI) = 2.411, t_0([5]) = 2.414) and for the temperature profile at this time (see Table 1). However, for the subsequent evolution to a warm steady-state there is a marked difference in the two models (see Table 1). The HBI model is close to the exact steady-state step solution whilst the exponential solution predicts temperature values some 10% higher.

For the hot steady-state ($\omega = 100\,000$, $Bi = 0.2$) the steady-state predictions of both models are once more very similar and agree with the exact profile (20) to

Table 1. Step HBI and numerical exponential [5] temperature predictions for a warm steady-state ($\varepsilon_1 = 2.78 \times 10^{-11}$, $\varepsilon_2 = 6.41 \times 10^{-9}$)

y	End of cold phase		Warm steady-state	
	Step HBI	[5]	Step HBI	[5]
0.0	1.0	1.0	$1+\varepsilon_1$	1.11656
0.2	0.99636	0.99656	0.99636	1.11055
0.4	0.98545	0.98617	0.98545	1.09328
0.6	0.96727	0.96870	0.96727	1.06676
0.8	0.94182	0.94390	0.94182	1.033376
1.0	0.90909	0.91144	0.90909	0.99529
	$t_0 = 2.411$	$t_0 = 2.414$	$t_\infty = t_0 + \varepsilon_2$	$t_\infty = 9.434$

Table 2. Step HBI and numerical exponential [5] temperature predictions for a hot steady-state ($\varepsilon_1 = 0.97 \times 10^{-5}$, $\varepsilon_2 = 1.0 \times 10^{-5}$)

y	End of cold phase		End of warm phase		Hot steady-state	
	Step HBI	[5]	Step HBI	[5]	Step HBI	[5]
0.0	1.0	1.0	1.1	2.21501	5.5	5.5
0.2	0.99636	1.00000	1.096	2.20581	5.48	5.48
0.4	0.98545	1.00000	1.084	2.17849	5.42	5.42
0.6	0.96727	1.00000	1.064	2.13400	5.32	5.32
0.8	0.94182	1.00000	1.036	2.07388	5.18	5.18
1.0	0.90909	1.00000	1.0	2.0	5.0	5.0
	$t_0 = \varepsilon_1$	$t_0 = \varepsilon_2$	$t_1 = 0.743$	$t_1 = 0.294$	$t_\infty = 101$	$t_\infty = 91$

seven decimal places. For this situation, both models prescribe an electrical conductivity g equal to δ. The steady-state times are different, $t_\infty(\text{HBI}) = 101$ and $t_\infty([5]) = 91$, and the routes taken to reach this point are quite different (see Table 2). Of course, the radical difference in the models concerns the warm stage which (a) has an exponentially varying electrical conductivity and (b) is defined over a fixed temperature range $U \in [1, 1+\Delta U]$.

In the limit as ΔU approaches zero, so the exponential model (2b) approaches the step function model (2a). However, there is a critical value of ΔU below which a numerical solution is extremely difficult, if not impossible, to obtain. It is precisely this case for which the HBI method works so well. For the general case $\Delta U > 0$, a purely numerical solution would appear to be the only tractable approach. Experiment shows that the critical value of ΔU to be about 0.11657, below which a numerical solution fails. Failure occurs in the sense that, as $\Delta U \to 0$, so extremely small time steps are required during the warm phase to satisfy the heuristic stability model discussed previously.

6. CONCLUSIONS

We have shown how a simple functional approximation can be used to model one particular thermistor problem. All the physical characteristics are satisfied and the vastly differing time scales and spatial scales of the problem are readily accounted for. Further, even with such a simple model (one-dimensional with constant potential difference), the solution process has extracted information which may support the idea that the cracks observed in some thermistors may be due to extremely rapid changes in temperature as opposed to large (spatial) temperature gradients. This is most likely to occur when the heating term ω is sufficiently large, resulting in a hot steady-state. This is in line with the temperature-surge hypothesis of Fowler *et al.* [5] who used the exponential conductivity model to obtain the asymptotic behaviour of the thermistor (including an external curcuit).

REFERENCES

1. E. D. Macklen, *Thermistors*. Electrochemical Publications, Ayr (1979).
2. D. Gelder and A. G. Guy, Current problems in the glass industry. In *Moving Boundary Problems in Heat Flow and Diffusion* (Edited by J. R. Ockendon and W. R. Hodgkins), pp. 71–90. Clarendon Press, Oxford (1975).
3. M. van der Veen, Thermistor cracking, 89-02, Technical University of Eindhoven Report (1989).
4. A. C. Fowler and S. D. Howison, Temperature surges in thermistors. In *3rd European Conference of Mathematics in Industry* (Edited by J. Manley *et al.*), pp. 197–204. Kluwer Academic, Stuttgart (1990).
5. A. C. Fowler, I. Frigaard and S. D. Howison, Temperature surges in current-limiting circuit devices, *SIAM J. Appl. Math.* **52**, 998–1011 (1992).
6. H. Diesselhorst, Über das Probleme eines elektrisch erwärmten Leiters, *Ann. Phys.* **1**, 312–325 (1900).
7. S. Howison, Complex variables in industrial mathematics. In *2nd European Symposium Mathematics in Industry* (Edited by H. Neunzert), pp. 153–166. Kluwer Academic, Stuttgart (1988).
8. S. Howison, A note on the thermistor problem in two space dimensions, *Q. Appl. Math.* **47**, 509–512 (1989).
9. G. Cimatti, Remark on existence and uniqueness for the

thermistor problem under mixed boundary conditions, *Q. Appl. Math.* **47,** 117–121 (1989).
10. G. Cimatti, A bound for the temperature in the thermistor problem, *Q. Appl. Math.* **40,** 15–22 (1988).
11. D. R. Westbrook, The thermistor: a problem in heat and current flow, *Numer. Meth. PDEs* **5,** 259–273 (1989).
12. A. S. Wood, Modelling the thermistor. In *5th European Conference Mathematics in Industry* (Edited by M. Heiliö), pp. 397–400. Kluwer Academic, Stuttgart (1991).
13. H. S. Carslaw and J. C. Jaeger, *Heat Conduction in Solids* (2nd Edn), p. 132. Clarendon Press, Oxford (1959).
14. G. G. Sackett, An implicit free boundary problem for the heat equation, *SIAM J. Numer. Anal.* **8,** 80–96 (1971).
15. T. R. Goodman, Applications of integral methods in transient non-linear heat transfer. In *Advances in Heat Transfer* (Edited by T. F. Irvive, Jr. and J. P. Harnett), Vol. 1, pp. 51–122. Academic Press, New York (1964).
16. D. S. Riley and P. W. Duck, Application of the heat balance integral method to the freezing of a cuboid, *Int. J. Heat Mass Transfer* **20,** 294–296 (1977).
17. A. S. Wood, An efficient finite-difference scheme for multidimensional Stefan problems, *Int. J. Numer. Meth. Engng* **23,** 1757–1771 (1986).
18. G. E. Bell, A refinement of the heat balance integral method applied to a melting problem, *Int. J. Heat Mass Transfer* **21,** 1357–1362 (1978).
19. L. H. van Vlack, *Physical Ceramics*, p. 152. Addison–Wesley, Massachusetts (1964).